

ANGPTL7, a therapeutic target for increased intraocular pressure and glaucoma

Kavita Praveen¹, Gaurang C. Patel², Lauren Gurski¹, Ariane H. Ayer¹, Trikaladarshi Persaud¹, Matthew D. Still², Lawrence Milosco¹, Tavé Van Zyl², Silvio Alessandro Di Gioia¹, Ben Brumpton^{3,4,5}, Kristi Krebs⁶, Bjørn Olav Åsvold^{3,4,7}, Esteban Chen¹, Venkata R. M. Chavali⁸, Wen Fury², Harini V. Gudiseva⁸, Sarah Hyde⁹, Eric Jorgenson¹, Stephanie Lefebvre⁹, Dadong Li¹, Alexander Li¹, James McIninch⁹, Brijeshkumar Patel², Jeremy S. Rabinowitz², Rebecca Salowe⁸, Claudia Schurmann¹⁰, Anne-Sofie Seidelin¹¹, Eli Stahl¹, Dylan Sun¹, Tanya M. Teslovich¹, Anne Tybjærg-Hansen¹¹, Cristen Willer^{12,13,14}, Scott Waldron⁹, Sabrina Walley², Hua Yang², Sarthak Zaveri², Regeneron Genetics Center*, GHS-RGC DiscovEHR Collaboration*, Estonian Biobank Research Team*, Ying Hu², Kristian Hveem^{3,4}, Olle Melander^{15,16}, Lili Milani⁶, Stefan Stender¹¹, Joan M. O'Brien⁸, Marcus B. Jones¹, Gonçalo R. Abecasis¹, Michael N. Cantor¹, Jonathan Weyne², Katia Karalis¹, Aris Economides^{1,2}, Giusy Della Gatta¹, Manuel A. Ferreira¹, George D. Yancopoulos², Aris Baras¹✉, Carmelo Romano²✉ & Giovanni Coppola¹✉

Glaucoma is a leading cause of blindness. Current glaucoma medications work by lowering intraocular pressure (IOP), a risk factor for glaucoma, but most treatments do not directly target the pathological changes leading to increased IOP, which can manifest as medication resistance as disease progresses. To identify physiological modulators of IOP, we performed genome- and exome-wide association analysis in >129,000 individuals with IOP measurements and extended these findings to an analysis of glaucoma risk. We report the identification and functional characterization of rare coding variants (including loss-of-function variants) in *ANGPTL7* associated with reduction in IOP and glaucoma protection. We validated the human genetics findings in mice by establishing that *Angptl7* knockout mice have lower (~2 mmHg) basal IOP compared to wild-type, with a trend towards lower IOP also in heterozygotes. Conversely, increasing murine *Angptl7* levels via injection into mouse eyes increases the IOP. We also show that acute *Angptl7* silencing in adult mice lowers the IOP (~2–4 mmHg), reproducing the observations in knockout mice. Collectively, our data suggest that *ANGPTL7* is important for IOP homeostasis and is amenable to therapeutic modulation to help maintain a healthy IOP that can prevent onset or slow the progression of glaucoma.

Glaucoma is a leading cause of irreversible blindness, with a global prevalence of 3.54% in individuals 40–80 years of age, and is projected to affect more than 111.8 million people by 2040¹. Classified as a neurodegenerative disease, glaucoma is characterized by the progressive loss of retinal ganglion cells in the eye and thinning of the neuroretinal rim of the optic nerve head. Affected individuals present with visual field loss that is accompanied by increased intraocular pressure (IOP) in the majority of cases². Primary open angle glaucoma (POAG) is the most common glaucoma subtype and has highest prevalence in individuals of African ancestry (4.2% prevalence in Africa¹).

Individuals at greatest risk for POAG are >60 years of age, have a family history of glaucoma, or have high myopia^{3–6}. Measurable ocular anatomical and physiological features, including low central corneal thickness (CCT), increased cup-to-disc ratio and high intraocular pressure (IOP)⁷ correlate with increased risk for glaucoma and, like glaucoma⁸, are highly heritable^{4,9–13}. Thus, these quantitative risk factors, when measured on large numbers of individuals, can provide a well-powered dataset for genetic studies to elucidate the etiology of glaucoma risk and progression. The latest genome-wide association study (GWAS) of IOP included more than 130,000 individuals and increased the tally of IOP-associated loci to over 100^{14,15}. An earlier GWAS¹⁶ reported that ~89% of loci associated with IOP at a genome-wide significant level showed directionally consistent effects on glaucoma risk, thus reinforcing the utility of quantitative risk factors in gene discovery for glaucoma.

Lowering IOP is the mainstay of all glaucoma therapeutics as IOP continues to be the only modifiable risk factor for the onset or progression of glaucoma. While many effective topical IOP-lowering agents across multiple drug classes are available, they have important drawbacks, including poor compliance due to frequent dosing requirements and side-effects¹⁷. Waning efficacy over time and the consequent need for treatment escalation are also observed, perhaps in part because the majority of medications in use do not address pathophysiological changes at the primary site of IOP regulation and aqueous humor egress from the eye, the trabecular meshwork (TM). These limitations result in a large proportion of glaucoma treatment regimens comprising more than one therapeutic agent and patients frequently changing medications or requiring treatment escalation that ultimately involves invasive surgery to maintain a clinically acceptable IOP¹⁸. Therefore, a substantial unmet need remains in the treatment of glaucoma to identify new therapeutic targets offering novel mechanisms of action, as well as treatment platforms that may offer increased durability and tolerability without compromising safety.

We performed genetic association analyses of IOP and glaucoma across eight cohorts to identify rare and coding variants that modulate the risk for glaucoma through IOP. This led to the identification of *ANGPTL7* as a candidate, consistent with findings reported recently by another group¹⁹. In this report, we (1) strengthen the genetic link to glaucoma protection by (i) showing a consistent protective effect of the Gln175His variant in *ANGPTL7* across eight cohorts, (ii) identifying a burden of ultra-rare missense variants in *ANGPTL7* associated with reduced IOP levels, and (iii) identifying an additional rare *ANGPTL7* loss-of-function variant in African-ancestry individuals; we also present (2) in vitro characterization of *ANGPTL7* variants identified from genetic analyses; and (3) in vivo results showing that mice lacking *Angptl7* have reduced basal IOP, and that even a partial knockdown of *Angptl7* with small interfering RNA (siRNA) can lead to lowering of IOP in mice. Our results establish an important role for *ANGPTL7* as a physiological regulator of IOP and suggest that it is also amenable to modification by pharmacological tools, making it a compelling target for a glaucoma therapeutic.

Results

Coding variants in *ANGPTL7* are associated with reduced IOP.

We studied the effect of rare, protein-altering variation on IOP across two large cohorts, UK Biobank (UKB) and the Geisinger DiscovEHR (GHS), including 129,207 individuals of European descent after exclusion of cases with a glaucoma diagnosis (Methods, Supplementary Table 1). To increase our power to detect associations with rare variants, we performed burden tests by aggregating for each gene all rare (minor allele frequency (MAF) < 1%) predicted loss-of-function (pLOF, defined as stop-gain, frameshift, splice donor, splice acceptor, start-loss, and stop-loss) and missense (predicted deleterious by 5 algorithms, Supplementary Methods) variants. We observed a genome-wide significant association ($P < 5 \times 10^{-8}$) of variants in angiotensin-like 7 (*ANGPTL7*) with reduced IOP ($\beta_{\text{allelic}} = -0.21$ SD, $P = 5.3 \times 10^{-24}$; Fig. 1a). The gene burden included 63 rare variants but was dominated by two: a missense (Gln175His, MAF = 0.7%) and a stop-gain (Arg177*, MAF = 0.03%) variant, which accounted for 1902 and 82 individuals out of a total of 2188 carriers, respectively (Figs. 1b, 2, Supplementary Fig. 1). Exclusion of Gln175His and Arg177* from the burden meta-analysis between UKB and GHS did not eliminate the signal completely ($\beta_{\text{allelic}} = -0.23$ SD, $P = 4.4 \times 10^{-4}$; Supplementary Fig. 2), suggesting that other ultra-rare variants in *ANGPTL7* are also associated with reduced IOP.

In single-variant analyses, Gln175His was associated with reduced IOP at a genome-wide significant level ($\beta_{\text{allelic}} = -0.20$ SD, $P = 3.1 \times 10^{-20}$, Fig. 2a). Heterozygous and homozygous carriers of Gln175His in *ANGPTL7* had a 5.2% (0.8 mmHg) and 26.5% (4.1 mmHg) reduction in median IOP in UKB, respectively (Fig. 2b). The Arg177* variant was also nominally associated with reduced IOP with an effect size similar to that of Gln175His ($\beta_{\text{allelic}} = -0.24$ SD, $P = 2.6 \times 10^{-2}$, Fig. 2c), and the 77 heterozygous Arg177* carriers had a 9% (1.4 mmHg) median IOP decrease (Fig. 2d). Arg177* appears to be the predominant pLOF variant in European populations; a burden test restricted to pLOF variants (15 variants across UKB and GHS) was dominated by Arg177* (82 of 112 total carriers) and was comparable ($\beta_{\text{allelic}} = -0.21$ SD, $P = 2.2 \times 10^{-2}$; Supplementary Fig. 3) to the single-variant association of Arg177* with IOP.

We searched other ancestries for additional pLOFs in *ANGPTL7* and identified Trp188*, which is enriched in individuals of African descent (MAF = 0.3%) compared to Europeans (MAF = 0.0013%). We performed an association of Trp188* with IOP in African ancestry individuals from UKB and the Primary Open Angle African American Glaucoma Genetics (POAAGG) study, followed by meta-analysis. Trp188* showed a trend towards reduced IOP, similar to Arg177* and Gln175His, but this was not statistically significant ($\beta_{\text{allelic}} = -0.11$ SD, $P = 5 \times 10^{-1}$). A cross-ancestry meta-analysis of Arg177* and Trp188* variants showed a nominally significant association with reduced IOP ($\beta_{\text{allelic}} = -0.21$ SD, $P = 1.5 \times 10^{-2}$; Supplementary Fig. 4).

In summary, we observed a significant association of Gln175His in *ANGPTL7* with reduced IOP and a sub-threshold association, in the same direction and of similar magnitude, with pLOF variants in *ANGPTL7*. Assuming the pLOF variants indeed cause a loss of protein function, our data suggest that loss of *ANGPTL7* can lead to lower IOP.

IOP-associated variants in *ANGPTL7* are protective against glaucoma. To understand if carriers of variants in *ANGPTL7* would also be protected against glaucoma, we performed an association analysis of Gln175His with glaucoma in UKB, GHS, and six additional studies: the Mount Sinai's BioMe Personalized

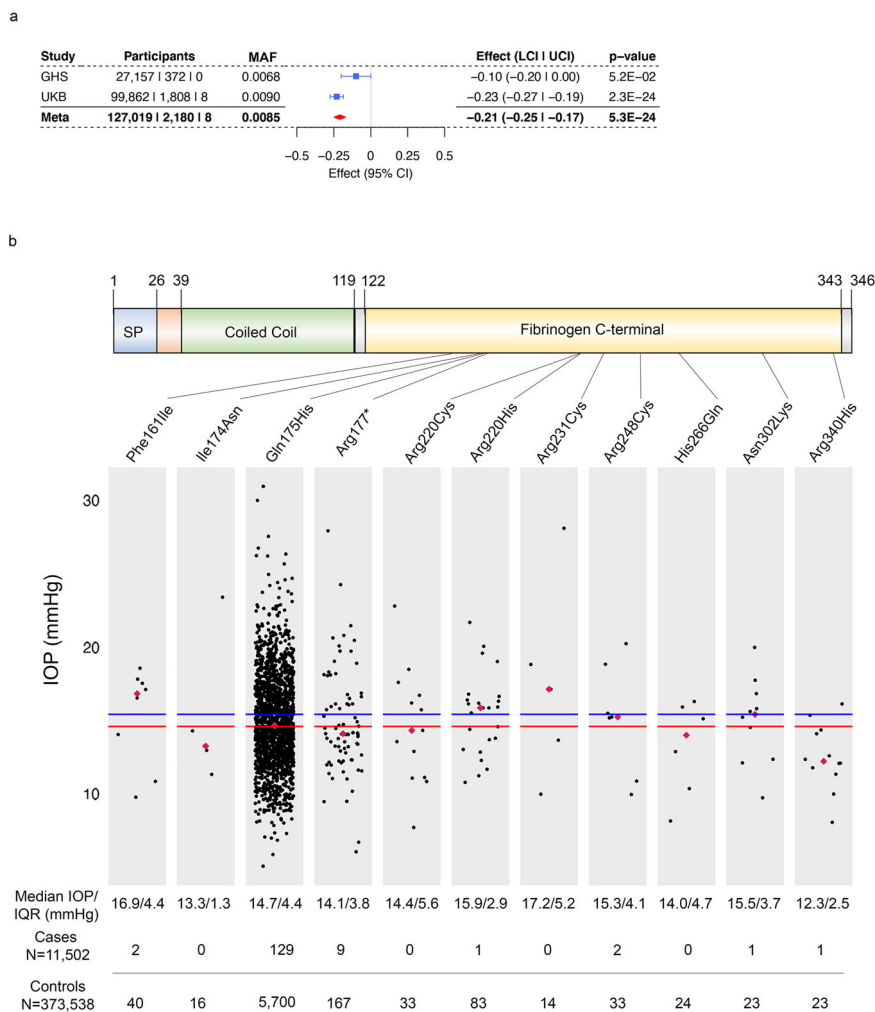


Fig. 1 An aggregate of rare (MAF < 1%) loss-of-function and missense variants in ANGPTL7 is associated with IOP. **a** Association of an aggregate of 63 pLOF and deleterious (based on 5 prediction algorithms) missense variants in *ANGPTL7* with reduced IOP in 129,207 individuals of European descent. **b** Missense and predicted loss-of-function (pLOF) variants in *ANGPTL7* and IOP levels in individuals of European descent from UKB. The plots represent Goldmann-correlated IOP (IOPg; mean of both eyes) levels in carriers of 1 pLOF and 10 missense variants in *ANGPTL7* that are predicted deleterious by five different algorithms and have at least five carriers amongst the 101,678 exome-sequenced individuals with IOP measurements in the UK Biobank. The median IOP level across carriers of all 49 pLOF and predicted-deleterious missense *ANGPTL7* variants (14.64 mmHg) is indicated by the red line, and the median IOP in non-variant carriers (15.46 mmHg) is indicated by the blue line. Magenta diamonds mark the median IOP in carriers of each variant. Beneath the plots is the median and interquartile range (IQR) of IOP and the numbers of variant carriers diagnosed with glaucoma or controls in UKB ($n = 385,040$). GHS Geisinger DiscovEHR, UKB UK Biobank, MAF Minor allele frequency.

Medicine Cohort from Mount Sinai Health System, New York (SINAI), the Malmö Diet and Cancer Study from Malmö, Sweden (MALMO), the FinnGen cohort from Finland, the Estonia Biobank at the University of Tartu, Estonia (EstBB), the HUNT study from Nord-Trøndelag, Norway (HUNT), and the Copenhagen General Population Study/Copenhagen City Heart Study from Copenhagen, Denmark (CGPS-CCHS). A meta-analysis across these eight cohorts showed a significant reduction in glaucoma risk for Gln175His carriers (odds ratio ($OR_{allelic}$) = 0.77, $P = 2.7 \times 10^{-6}$, Fig. 3a). We also analyzed glaucoma risk in carriers of the rarer Arg177*/Trp188* variants in a cross-ancestry meta-analysis and observed a consistent trend towards reduction in risk ($OR_{allelic} = 0.87$, $P = 4.1 \times 10^{-1}$, Fig. 3b). Taken together, the associations of missense and pLOF variants in *ANGPTL7* with reduced IOP and the association of the missense variant with reduced glaucoma risk suggest the hypothesis that loss of *ANGPTL7* confers protection against glaucoma, and that this effect is mediated through the regulation of IOP.

ANGPTL7 variants are associated with corneal measures. We performed a phenome-wide association analysis (PheWAS) to understand whether other traits were associated with a burden of pLOF and deleterious missense variants in *ANGPTL7*. We tested the *ANGPTL7* variant aggregate for association with 14,050 and 10,032 binary and quantitative traits in UKB and GHS, respectively. No associations reached phenome-wide significance ($P < 2 \times 10^{-6}$ after multiple-testing correction for 24,082 total traits) in GHS. The only significant associations in UKB were with ocular traits (Table 1), specifically with decreased corneal-compensated IOP (IOPcc), decreased corneal resistance factor (CRF) and increased corneal refractive power along both weak and strong meridians measured at 3 and 6 mm diameters. The effect of these variants on IOPcc was slightly attenuated (-0.17 SD) compared to that on IOPg (-0.23 SD in UKB), which suggests that *ANGPTL7* has some impact on corneal properties that are known to affect the IOPg measurements²⁰. The association observed with decreased CRF is also consistent with a corneal effect of *ANGPTL7*.

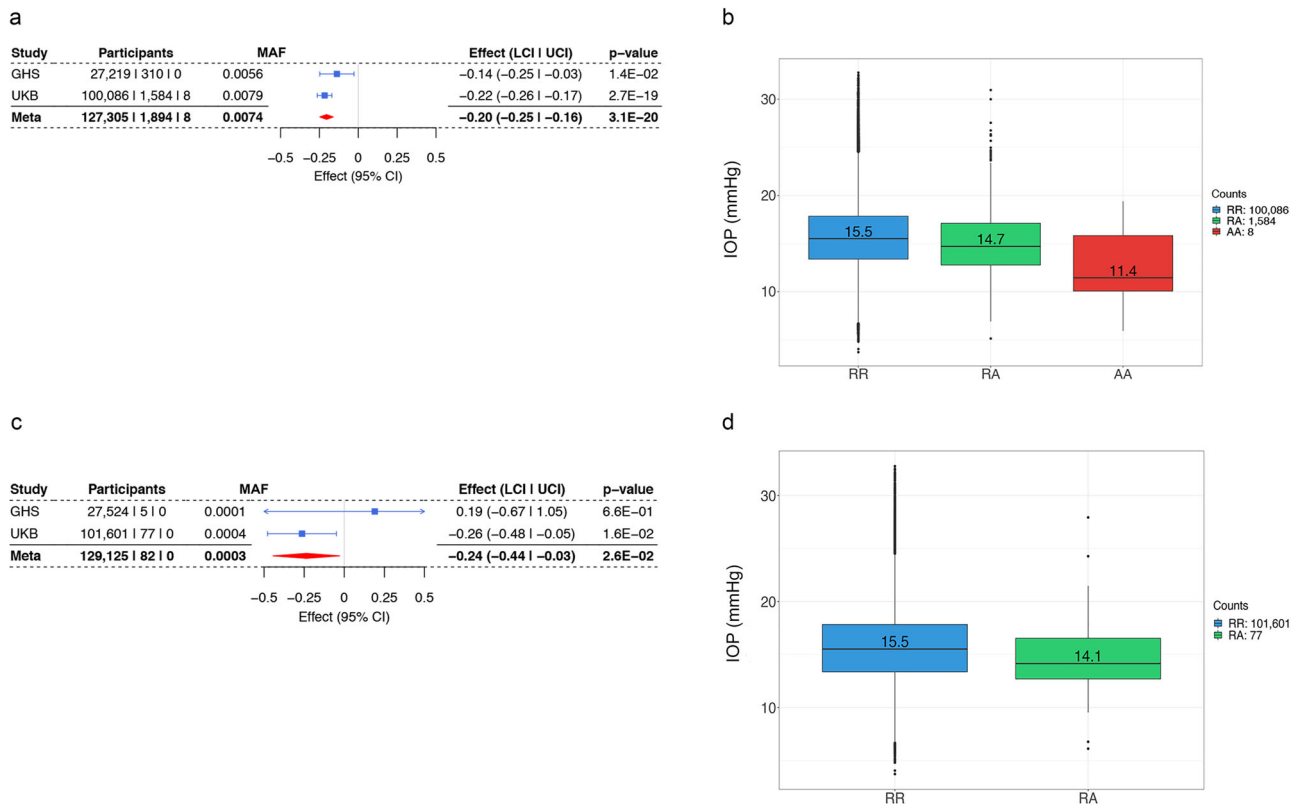


Fig. 2 Gln175His and Arg177* are major contributors to the gene burden association of *ANGPTL7* with IOP. Association of Gln175His (**a**) and Arg177* (**c**) variants in *ANGPTL7* with IOP, effect measured in standard deviation units, in individuals of European descent. **b, d** Boxplots representing IOPg in the UK Biobank across genotypes. **b** Gln175His heterozygous and homozygous carriers have a 0.8-mmHg and 4.1-mmHg lower median IOPg, respectively, compared to non-carriers. **d** Arg177* heterozygous carriers have a 1.4-mmHg lower IOPg compared to non-carriers. GHS Geisinger DiscovEHR, UKB UK Biobank, MAF Minor allele frequency.

We used the autorefractometry measurements at 3 mm diameter to derive measures of clinical interest, namely, mean corneal refractive power (mCRP), corneal astigmatism, and refractive astigmatism (Supplementary Methods) and checked for association with *ANGPTL7*. We observed a significant association with increased mCRP ($\beta_{\text{allelic}} = 0.16$ SD, $P = 1.1 \times 10^{-13}$, Table 1) but no association with corneal or refractive astigmatism. We also did not observe associations with mean spherical equivalent (MSE; measure of refractive error) or myopia (either derived from MSE or via ICD-10 diagnosis), which could result from increased mCRP (Supplementary Table 2). Overall, our PheWAS results show that while *ANGPTL7* is associated with changes in corneal anatomy/biomechanics-related quantitative measures, we did not detect an increased risk for any related disease outcomes that we could test. In addition, pLOF and deleterious missense variants in *ANGPTL7* are not associated with any systemic quantitative traits or binary outcomes.

Gln175His, Arg177* and Trp188* are defective in secretion. To understand the impact of Gln175His, Arg177*, and Trp188* variants on the expression and secretion of *ANGPTL7*, we transiently transfected constructs expressing the human wild type (WT), Gln175His, Arg177*, and Trp188* proteins in HEK293 cells. We measured mRNA levels by Taqman, which showed similar Gln175His and Arg177* transcript levels and a trend towards decreased levels of the Trp188* transcript compared to WT ($P = 0.08$; Supplementary Fig. 5). However, analysis of intracellular, steady-state protein in whole-cell lysate by western blotting and ELISA revealed increased levels of Gln175His compared to WT ($P < 1 \times 10^{-4}$; Fig. 4c). As expected, Arg177*

and Trp188* encoded lower molecular weight proteins (~30–32 kDa). No significant difference in the protein levels of these two mutants was revealed by ELISA in comparison to WT (Fig. 4a, c). Because *ANGPTL7* is a secreted protein, we next determined the levels of WT, Gln175His, Arg177*, and Trp188* in the cellular supernatant. Protein analysis by western blot showed that the Arg177* and Trp188* variants were not detectable and the Gln175His was drastically reduced in the supernatant compared to WT ($P < 0.05$; Fig. 4b). ELISA assay further corroborated the severely reduced levels of Gln175His and the inability of Arg177* and Trp188* to reach the extracellular space (Fig. 4c, d).

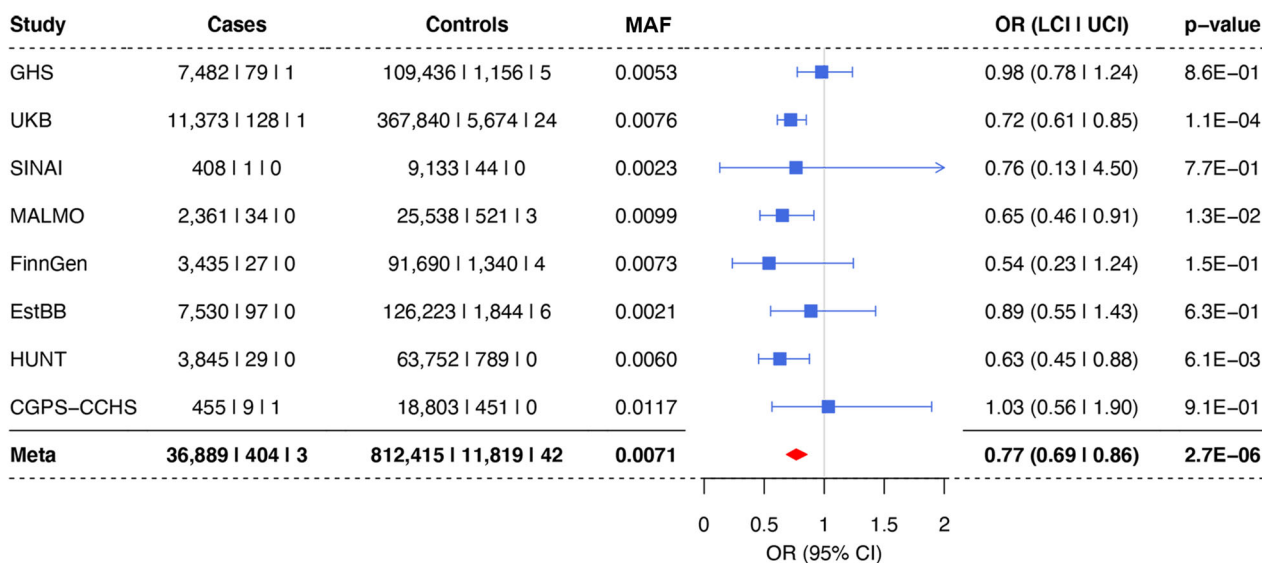
***ANGPTL7* is expressed in cornea, TM and sclera across species.**

To identify expression of *ANGPTL7* in ocular tissues across different species, transcriptome profiles from different parts of the eye were generated (Supplementary Methods). High *ANGPTL7* expression was observed in cornea, TM, and sclera in human and African green monkey eyes (Fig. 5a, b, Supplementary Fig. 6). High *Angptl7* expression was also observed in cornea, TM, sclera, optic nerve head, and choroid/RPE in eyes of C57BL/6J mice (Fig. 5c). In situ hybridization on human donor and mouse eyes using RNAscope probes for human *ANGPTL7* and mouse *Angptl7* showed *ANGPTL7/Angptl7* expression in TM, cornea stroma, and sclera (Fig. 5d, e; Supplementary Methods).

Increasing levels of mAngptl7 in mouse eyes increases IOP.

Previous studies showed that overexpression of *ANGPTL7* in TM cells leads to changes in extracellular matrix (ECM) deposition

a



b

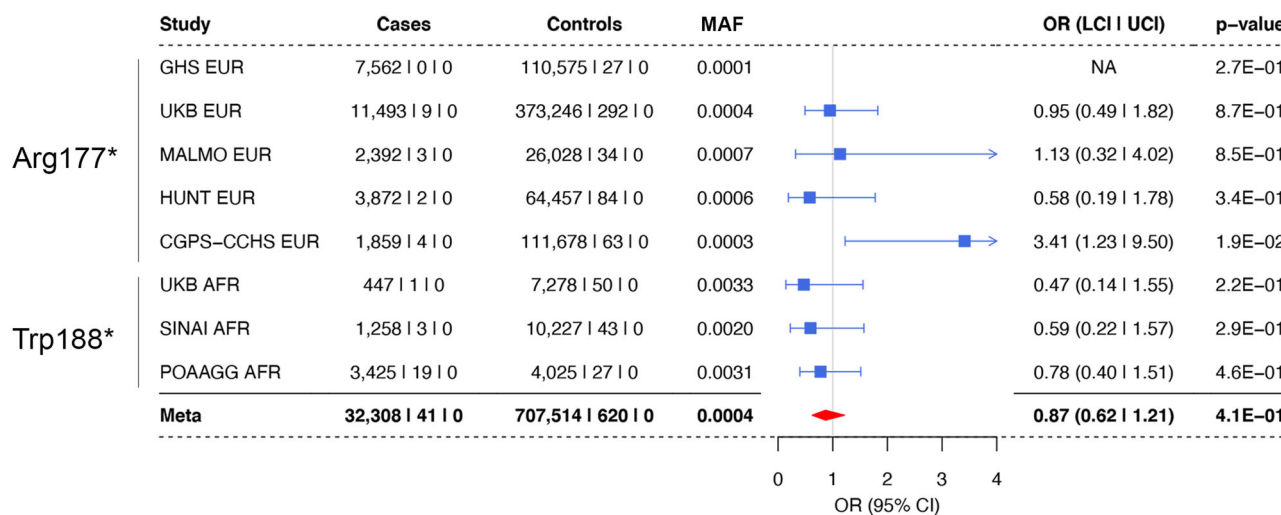


Fig. 3 Association of ANGPTL7 variants with glaucoma. a Meta-analysis results for Gln175His with glaucoma across 8 different cohorts. **b** Cross-ancestry meta-analysis of Arg177* and Trp188* across 5 European (EUR) and 3 African (AFR) ancestry cohorts. The variants in the meta-analysis of EUR and AFR cohorts were Arg177* and Trp188*, respectively. GHS Geisinger DiscovEHR, UKB UK Biobank, SINAI Mt. Sinai Medical School BioMe Biobank, MALMO Malmö Diet and Cancer Study, EstBB the Estonia Biobank at the University of Tartu, HUNT the HUNT study from Nord-Trøndelag, CGPS-CCHS the Copenhagen General Population Study and the Copenhagen City Heart Study, POAAGG Primary Open Angle African-American Glaucoma Genetics, MAF Minor allele frequency.

and reorganization^{21,22} and that ANGPTL7 is increased in aqueous humor of glaucoma patients²², however, the role of ANGPTL7 in IOP regulation is not clear. To investigate this, we injected mAngptl7 protein in mice via intravitreal and intracameral routes and measured IOP over time. Intravitreal injection of murine Angptl7 (mAngptl7) in mice led to an initial drop in IOP followed by, starting on day 4, an elevation in IOP of 4–5 mmHg, a 22–25% increase compared to baseline, that lasted until the end of the experiment on day 7 (Fig. 6a). Similarly, intracameral injection of mAngptl7 in mice led to an initial drop and subsequent elevation (by 2–5 mmHg) of IOP, starting on day 3 until the end of the experiment on day 7 (Fig. 6b). Vehicle-

injected mice did not show an increase in IOP in either route of administration.

Angptl7 KO mice have lower basal IOP than WT. We generated and characterized *Angptl7*^{-/-} (KO) mice. We confirmed via RNAscope that *Angptl7* mRNA was not expressed in any ocular tissue in KO mice whereas it was expressed in TM, cornea, and sclera of WT mice (Fig. 7; Supplementary Methods). In addition, histological analysis of the eye showed no difference in the ocular angle in KO mice compared with WT (Supplementary Fig. 7). We did not observe any ocular changes on anterior segment optical

Table 1 Statistically significant ($P < 2 \times 10^{-6}$) results from PheWAS of an aggregate of up to 110 pLOF and deleterious missense variants (MAF < 1%) in *ANGPTL7* in UKB.

Trait	P value	OR/Effect in SD (LCI UCI)
Corneal-compensated intraocular pressure (IOPcc) (mean of both eyes)	6.32E-14	-0.17 [-0.21 -0.13]
CRF (right eye)	5.20E-13	-0.16 [-0.20 -0.11]
CRF (left eye)	4.50E-12	-0.15 [-0.20 -0.11]
6 mm weak meridian (left eye)	4.00E-20	0.21 [0.16 0.25]
6 mm weak meridian (right eye)	4.20E-18	0.19 [0.15 0.24]
6 mm strong meridian (left eye)	3.10E-17	0.19 [0.14 0.23]
6 mm strong meridian (right eye)	7.60E-17	0.18 [0.14 0.23]
3 mm weak meridian (right eye)	2.00E-14	0.16 [0.12 0.20]
3 mm weak meridian (left eye)	1.60E-13	0.15 [0.11 0.20]
3 mm strong meridian (left eye)	1.30E-12	0.15 [0.11 0.19]
3 mm strong meridian (right eye)	1.80E-12	0.15 [0.11 0.19]
Corneal power (mean of both eyes)	1.10E-13	0.16 [0.11 0.20]

CRF Corneal resistance factor.

coherence tomography, or a difference in corneal thickness between the two genotypes (Supplementary Fig. 8). We also monitored the IOP in KO, *Angptl7*^{+/-} (Het) and WT mice and observed a dose-dependent decrease in IOP across the three genotypes (Fig. 8a). The mean IOP was lowered in KO mice (mean \pm standard error of the mean (SEM): 15.39 ± 0.25 mmHg) by 11% (1.96 mmHg, $P < 1 \times 10^{-4}$) compared to WT (17.36 ± 0.23 mmHg). Het mice (16.26 ± 0.43 mmHg) showed a smaller (6%, 1.1 mmHg, $P = 0.02$) but significant reduction in IOP compared to WT.

Angptl7 KO mice have increased conventional outflow facility.

Angptl7 is highly expressed in cornea and TM and since we used a Tonolab rebound tonometer to measure IOP, we wanted to further confirm that *Angptl7* function in the cornea was not affecting IOP. Therefore, we measured the conventional outflow facility using constant flow infusion to understand the relationship between IOP and outflow resistance in *Angptl7* KO ($n = 7$) and WT mice ($n = 4$). The conventional outflow facility was increased by 21% in KO (25.18 nL/minute/mmHg) compared to WT mice (20.85 nL/minute/mmHg; $P = 0.15$; Fig. 8b). The mean increase in outflow facility was consistent with the mean IOP lowering in KO, according to the modified Goldman equation.

siRNA-induced knockdown of *Angptl7* mRNA and lowering of IOP in WT Mice.

To investigate whether knockdown of *Angptl7* with siRNA can also lower IOP, we tested six different siRNAs (Table 2) targeting *Angptl7* in C57BL/6J mice and monitored IOP over time. We injected C57BL/6J mice intravitreally with $15 \mu\text{g}$ of siRNAs and performed qPCR six weeks later on limbal rings dissected from mouse eyes enriched for the TM. IOP was significantly lowered two weeks post-injection in mice treated with two of the six siRNAs (siRNA #3 and #5) compared to the PBS and Naïve (no injection) groups (Fig. 8c, Supplementary Data 1). Naïve and PBS-treated animals maintained their IOPs at baseline for the duration of the study (weeks 0–6). In mice treated with siRNA#3 and #5, IOP was lowered by 2–4 mmHg starting at week 2 compared to PBS-treated mice (Fig. 8c). At the end of the study, we collected the eyes, carefully micro-dissected the limbal ring and performed qPCR. We observed the highest level of knockdown (>50%) of *Angptl7* mRNA with siRNAs #3 and #5 compared to PBS-treated mice (Fig. 8d), which is consistent with

the IOP lowering observed in mice injected with these two siRNAs. These results suggest that acute inhibition of *Angptl7* expression also lowers IOP.

Discussion

In this study, we present genetic and functional evidence for a role for *ANGPTL7* in the physiological control of IOP and as a potential target for glaucoma therapy. A recent publication by Tanigawa et al.¹⁹ identified a protective association of *ANGPTL7* with glaucoma and in this paper we further evaluate and strengthen this finding by (1) adding six cohorts to the genetic association analyses in UK Biobank and FinnGen that were used in Tanigawa et al, and showing a consistent protective trend in the majority of these for the rare missense variant, Gln175His (rs28991009); (2) identifying an African ancestry-enriched pLOF variant, Trp188*, in *ANGPTL7* in addition to Arg177* in Europeans and showing that both variants trend towards protection from glaucoma (3) identifying through exome sequencing and gene burden analyses multiple predicted-deleterious *ANGPTL7* variants associated with reduced IOP, indicating that there may be other ultra-rare *ANGPTL7* variants that confer protection from glaucoma. Together, these new analyses provide further support for the role of *ANGPTL7* in IOP regulation and glaucoma pathogenesis. We also show through cell-based expression assays, that Gln175His, Arg177*, and Trp188* were severely defective in secretion when compared to wild-type and, while not proof, this observation is consistent with the hypothesis that the three variants result in a loss of protein function.

ANGPTL7 is a secreted glycoprotein that is thought to form homo-oligomers (tri- or tetramers), like other members of the *ANGPTL* family^{23,24}. The *ANGPTL7* mRNA was first isolated from human postmortem eyes where it shows the highest expression relative to other tissues²³. Within the eye, our in situ hybridization results show that *ANGPTL7* is expressed most strongly in the cornea and TM, consistent with previous findings²². We have also shown using single-cell RNAseq that *ANGPTL7* expression is particularly enriched in the juxtacanalicular tissue (JCT), a region of the TM most important for IOP regulation and generation of aqueous humor outflow resistance^{25,26}. In addition to being expressed in tissues directly relevant in glaucoma, several lines of evidence have implicated *ANGPTL7* in glaucoma pathophysiology. First, elevated levels of *ANGPTL7* mRNA and protein were observed in eye tissues from glaucoma patients compared to controls, and under conditions of increased IOP simulated by perfusion of eye anterior segment explants^{22,27,28}. Second, *ANGPTL7* is one of the most upregulated genes in response to corticosteroid treatment^{29,30}, which can cause increased IOP in ~40% of general population and ~90% of individuals with POAG^{31,32}. Third, *ANGPTL7* levels are also increased in response to TGF-beta, a growth factor that is thought to modulate the ECM and lead to increased IOP³³. Fourth, *ANGPTL7* itself can modulate the expression of components of the TM ECM^{21,22}.

The above studies suggest a strong correlation of *ANGPTL7* expression with glaucoma disease-state, however, they are not evidence for a causal relationship between *ANGPTL7* levels and elevated IOP/glaucoma. Human genetics finding of an association between *ANGPTL7* loss and lower IOP suggests that *ANGPTL7* is physiologically important for IOP regulation. We validated this hypothesis in mice where we performed reciprocal experiments: measuring IOP after increasing *ANGPTL7* levels via injection of m*Angptl7* into mouse eyes, and after removing all m*Angptl7* protein by generating *Angptl7* KO mice. Our findings show that increasing m*Angptl7* results in increased (~2–4 mmHg) IOP and decreasing m*Angptl7* through KO mice

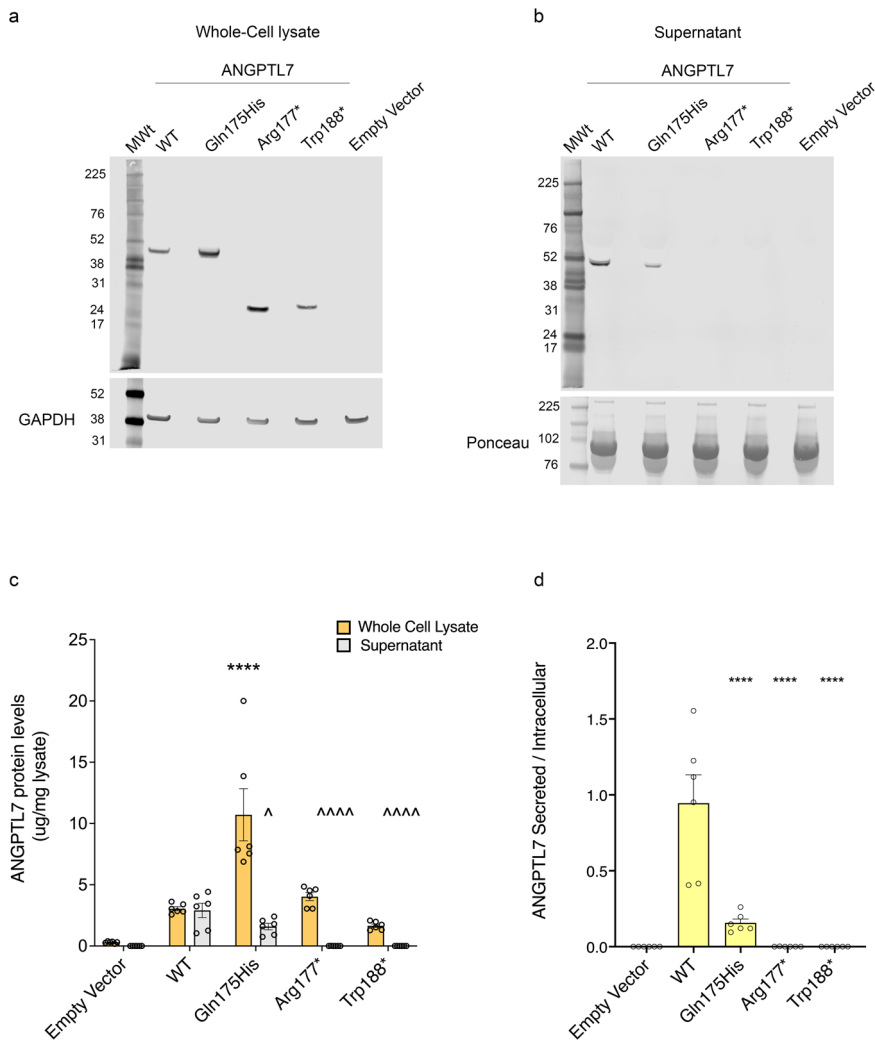


Fig. 4 Expression analysis of ANGPTL7 Gln175His, Arg177*, and Trp188* in a HEK293 cell line. **a, b** Western blotting shows intra- and extra-cellular protein levels of ANGPTL7 wild-type (WT), Gln175His, Arg177*, and Trp188*. **c** ELISA was run to quantify intra- and extra-cellular protein levels of ANGPTL7 WT, Gln175His, Arg177*, and Trp188* transiently transfected in HEK293 cells (whole-cell lysate was diluted 1:1,000; supernatant was diluted 1:10,000. Both whole-cell lysate and supernatant were normalized against the total amount of protein from the whole-cell lysate); **** = $P < 1 \times 10^{-4}$ statistical difference from WT whole cell lysate; ^ = $P < 0.05$, ^^^ = $P < 1 \times 10^{-4}$ statistical difference from WT supernatant. **d** Ratio of secreted versus intracellular ANGPTL7 WT, Gln175His, Arg177*, and Trp188* protein levels. Raw ANGPTL7 WT, Gln175His, Arg177*, and Trp188* protein levels were normalized to the whole-lysate protein concentration; **** = $P < 1 \times 10^{-4}$ statistical difference from WT. Western blotting and ELISA analysis were repeated on three independent biological replicates. Technical replicates ($n = 3$) were run for the ELISA analysis. P values were calculated by one-way ANOVA with Tukey's post hoc analysis. All data are presented as mean and error bars indicate the standard error of the mean (SEM). MWt molecular weight marker.

reduces basal IOP levels (~2 mmHg). We also observed a trend towards increased conventional outflow facility (~21%) in KO compared to WT mice that was consistent with the decrease in IOP in KO mice. Together, these findings suggest that ANGPTL7 functions in vivo to maintain IOP homeostasis. We further recapitulated the reduction in IOP observed in KO mice by injecting WT mouse eyes with siRNA against *Angptl7*, which not only replicates the observation in genetic mutant mice but also illustrates that the effect of mAngptl7 on IOP continues post-development and is amenable to modulation by therapeutics in adulthood. Our results of lower IOP in *Angptl7* KO mice are highly consistent with observations from human genetics. Based on this, we could extend the siRNA knockdown findings to humans and surmise that inhibition of ANGPTL7 in adulthood could be an efficacious strategy to lower IOP and, eventually, the risk for glaucoma.

Our human genetics findings indicate that the variants in *ANGPTL7* associated with reduced IOP were also associated

with decreased mean corneal resistance factor (CRF), an output of the Ocular Response Analyzer that reflects the elastic property of the cornea³⁴, and increased mean corneal refractive power (mCRP). mCRP, along with axial length and lens power, contributes to the overall refractive state of the eye³⁵, and increased mCRP (i.e. a steeper cornea) may be indicative of possible myopia or astigmatism. However, as we did not observe evidence of association with myopia or astigmatism in PheWAS, we conclude that the changes to mCRP are either insufficient to result in a disease outcome or are compensated by other changes in traits that were not measured, such as axial length³⁶. While an effect of ANGPTL7 on corneal properties is clearly indicated by the associations with mCRP and CRF, we assert that this effect cannot account for the full extent of IOP reduction observed. Instead, we posit an independent contribution of ANGPTL7 to IOP homeostasis based on the following: (1) The persistent association with reduced IOPcc suggests that there is IOP reduction even after controlling for

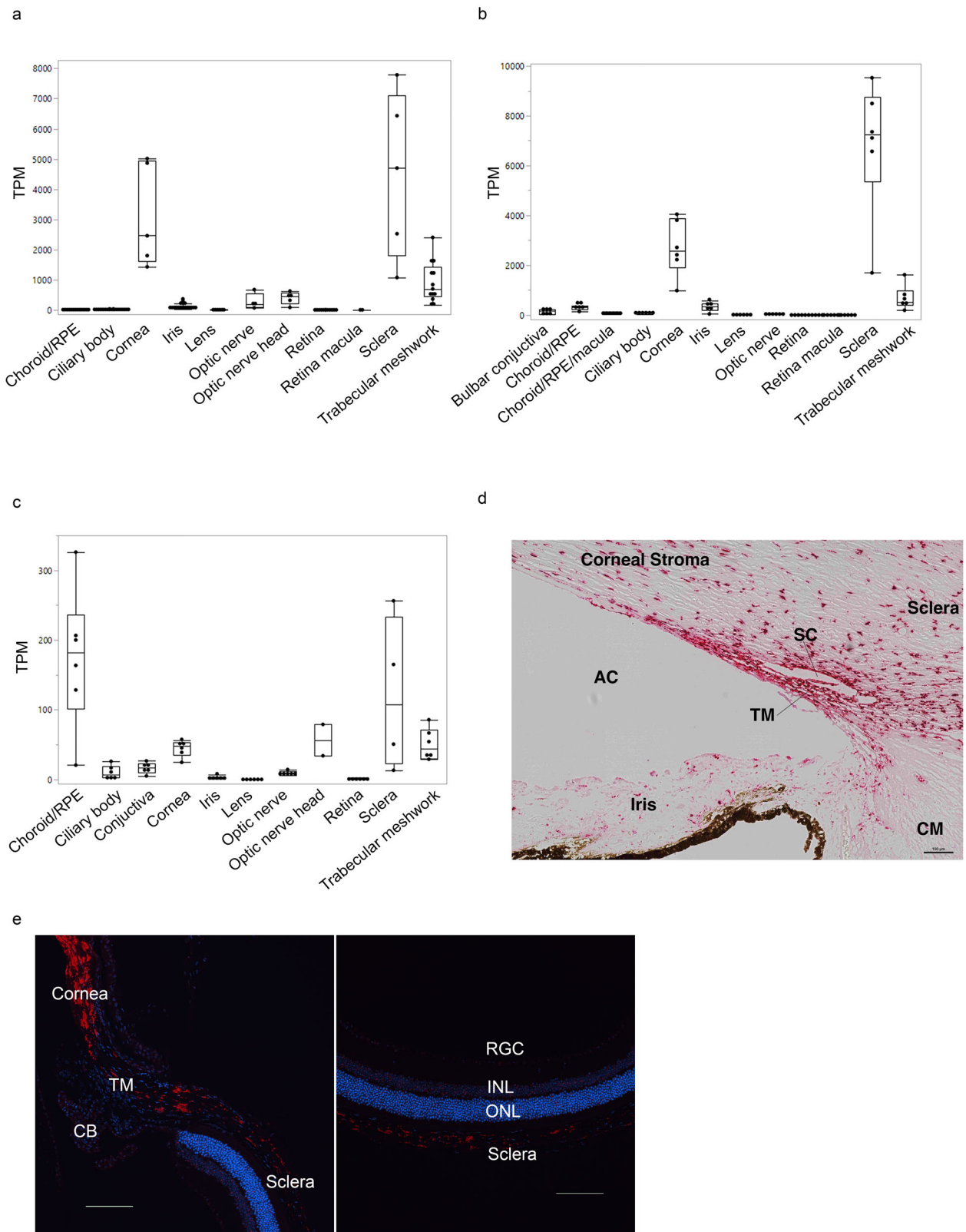


Fig. 5 ANGPTL7 expression in ocular tissues across species. RNA-sequencing-based expression levels (measured in transcripts per million, TPM, and represented as median and interquartile range) are highest in cornea, trabecular meshwork (TM), and sclera in human (**a**), and African green monkey (**b**) eyes, and in cornea, TM, sclera, optic nerve head, and choroid/RPE in C57BL/6 J mouse eyes (**c**); In situ hybridization (RNAscope) shows *ANGPTL7*/ *Angptl7* (red) expression in TM, cornea and sclera in human (**d**) and murine (**e**) eyes. Scale bars represent 100 μ m. DAPI staining (blue) counterstains cell nuclei. RPE retinal pigmented epithelium, CB ciliary body, SC Schlemm’s canal, CM ciliary muscle, AC anterior chamber, RGC retinal ganglion cell, INL inner nuclear layer, ONL outer nuclear layer.

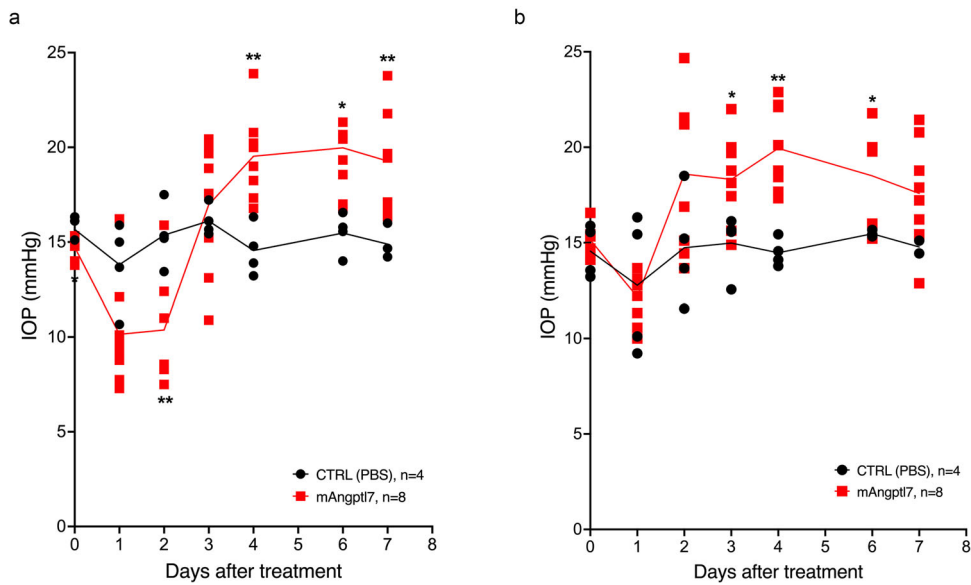


Fig. 6 Increasing mAngptl7 levels in mouse eyes increases IOP. Murine Angptl7 (mAngptl7) protein was injected into mouse eyes via intravitreal (a) or intracameral route (b), and IOP was measured over time. After an initial drop, IOP remained elevated for several days in mAngptl7-treated eyes compared to PBS treated (CTRL (PBS)) eyes. * = $P < 0.05$; ** = $P < 0.01$ statistical significance compared to PBS treatment. Statistical analyses were performed using Student’s *t* test.

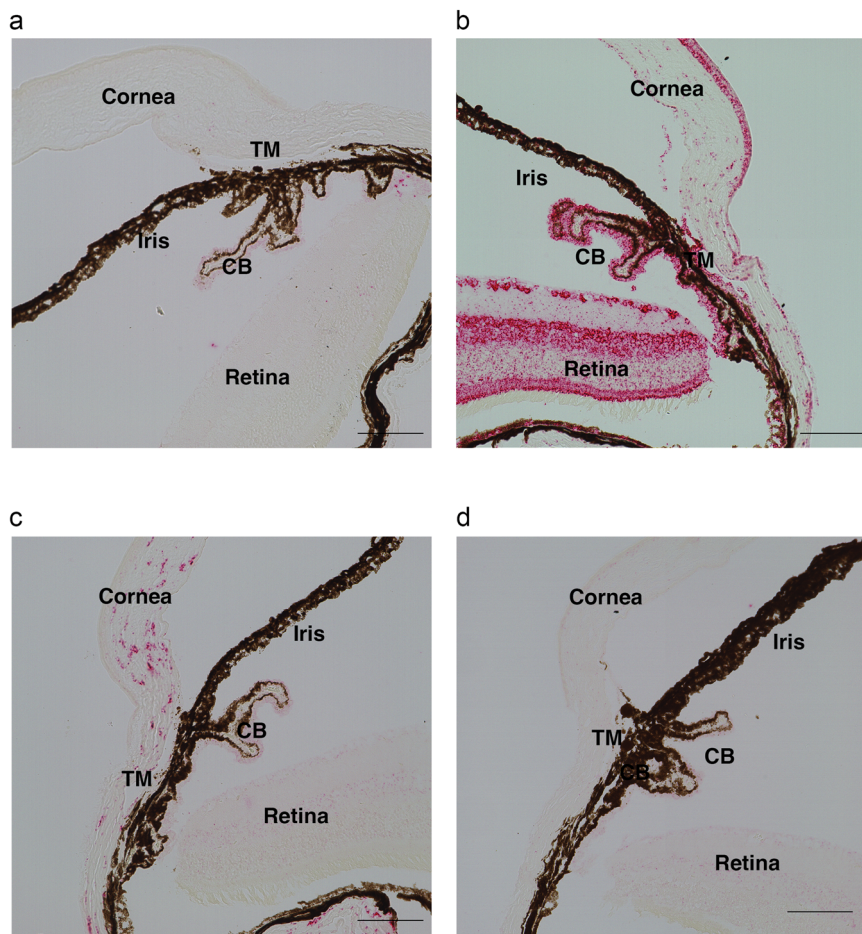


Fig. 7 In situ characterization of Angptl7 mRNA in WT and *Angptl7* KO mouse eyes. Angptl7 mRNA was not expressed in any ocular tissue in *Angptl7* KO mice whereas it was expressed in TM, cornea, and sclera of WT mice as shown by in situ hybridization (RNAscope). Brightfield images showing following probes. **a** Negative control: DapB. **b** Positive control: Ubc (red). **c** WT mice: Angptl7 (red), and **(d)** *Angptl7* KO mice: Angptl7 (no signal). Scale bars represent 100 μm.

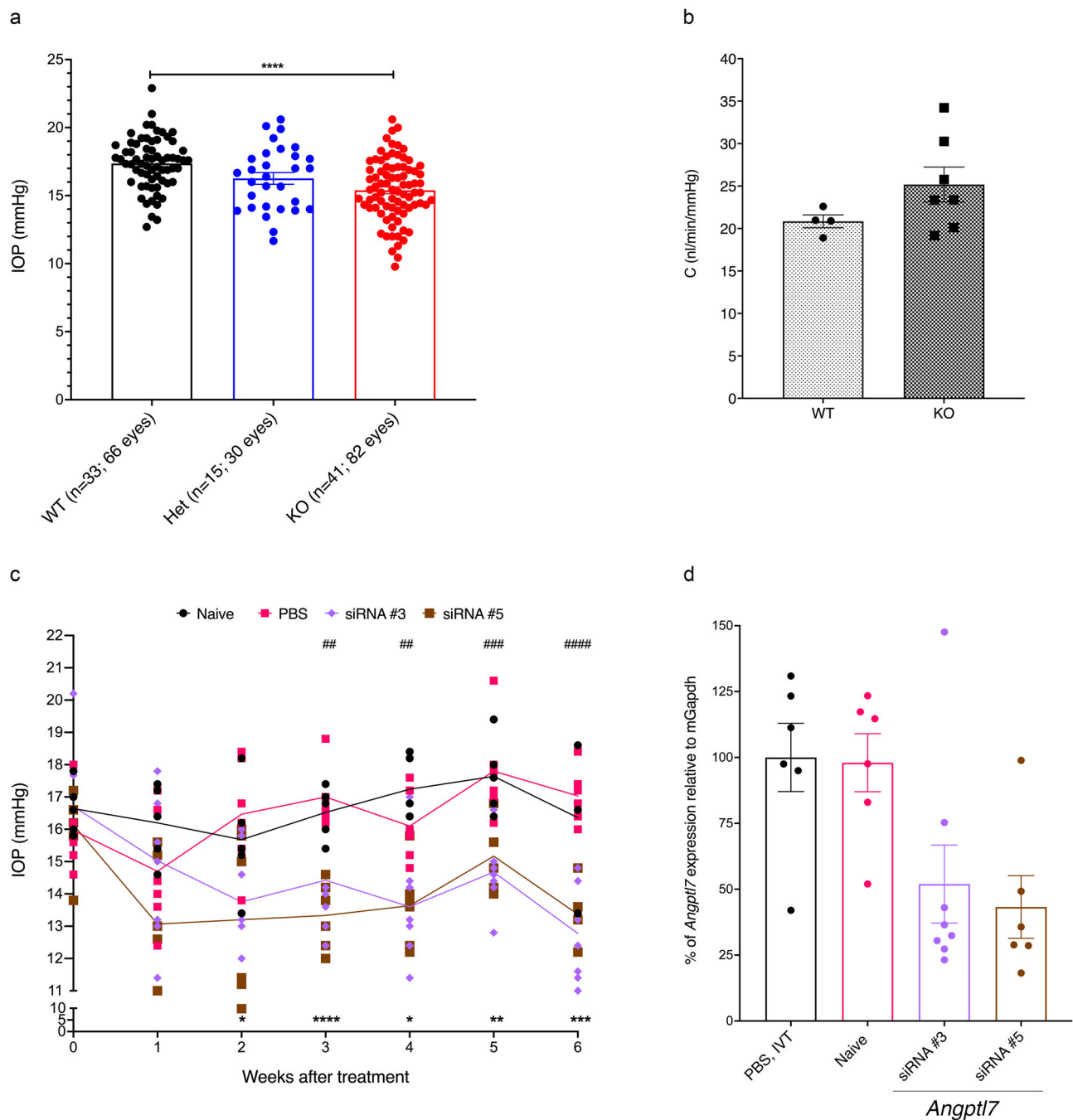


Fig. 8 Reducing mAngptl7 levels in mice lowers IOP. **a** IOP was significantly lowered in *Angptl7* KO compared to Het and WT mice (mean \pm SEM; **** = $P < 1 \times 10^{-4}$). **b** Comparison of conventional outflow facility (C) between KO and WT mice. In KO mice ($n = 7$), C was increased compared to WT mice ($n = 4$, $P = 0.16$, unpaired Student's *t* test). Data are presented as mean \pm SEM. **c** Intravitreal injection with 15 μ g of *Angptl7*-siRNA significantly lowered IOP in two of six siRNAs tested ($n = 6-8$ /group) compared to the PBS ($n = 6$) and Naive (no injection, $n = 5$) groups and remained lowered throughout the end of the study. siRNAs 3 and 5 lowered IOP between 2 and 4 mmHg starting at week 2 compared to PBS-treated mice. * = $P < 0.05$, ** = $P < 0.01$, *** = $P < 1 \times 10^{-3}$, **** = $P < 1 \times 10^{-4}$ statistical difference between the mean IOP for siRNA #5 and PBS-treatment. # = $P < 0.05$, ## = $P < 0.01$, ### = $P < 1 \times 10^{-3}$, #### = $P < 1 \times 10^{-4}$ statistical difference between the mean IOP for siRNA #3 and PBS-treatment. **d** qPCR results from micro-dissected limbal ring showed the highest level of knockdown (>50%) of *Angptl7* mRNA with siRNAs #3 and #5 compared to PBS-treated mice, which is highly consistent with the IOP lowering observed in mice injected with these two siRNAs (**b**). Data are presented as mean and error bars represent SEM.

corneal properties; (2) *Angptl7* KO mice eyes show reduced basal IOP without evidence of corneal thinning or other corneal abnormalities; and (3) the association of *ANGPTL7* variants with glaucoma protection is a result we would not expect if the reduction of IOP was purely due to *ANGPTL7*'s effect on

corneal anatomy³⁷. Therefore, we believe that *ANGPTL7* likely has a pleiotropic effect on both IOP and corneal anatomy/biomechanics in humans.

Therapeutic knockdown of *ANGPTL7* in patients with open angle glaucoma may present a unique opportunity to not only

Table 2 Mouse Angptl7 siRNA sequences used to knockdown mAngptl7.

siRNA	sense strand	antisense strand
#1	UUGGGCAAUGAACUGAACAGA	UCUGUUCAGUUCUUGCCCAACG
#2	GUACCAGAAGAACUACCGAAA	UUUCGGUAGUUCUUCUGGUACAG
#3	AGACAGUUAAGCAAGGGUUA	UAACCCUUGCUUAUACUGUCUCC
#4	GCAGAAGCCUCAUAACGCAA	UUGCGUUUAGAGGCUUCUGCAG
#5	ACACUCCUUGUGUCUAUAGA	UCUAUAGACACAAGGAAGUGUCG
#6	CUGCAGAAGCCUCAUAACGA	UCGUUUUAGAGGCUUCUGCAGCC

lower IOP through a novel mechanism of action, but also to intervene in the disease process. Among the most widely used IOP-lowering agents, none directly address pathophysiological changes occurring at the level of TM and instead reduce IOP through mechanisms that reduce the aqueous burden on the conventional pathway, either through suppressing aqueous formation or increasing its outflow via the alternative (uveoscleral) pathway³⁸. Consequently, as TM dysfunction progresses in a glaucoma patient, treatment intensification naturally follows¹⁸. While further studies are needed to investigate the role of ANGPTL7 in pathways contributing to TM dysfunction and IOP elevation, several lines of evidence point to pro-fibrotic actions at the level of the TM, including its corticosteroid and TGF- β responsiveness, as well as its enriched expression in JCT TM (discussed earlier).

As all studies, this study has limitations. First, we did not account for IOP-lowering medication use in the IOP analysis. We did exclude from the IOP analysis individuals with a glaucoma diagnosis, greatly reducing the effect of medication use, however this would not exclude those individuals on IOP-lowering medications without a glaucoma diagnosis. In addition, the IOP measurement in UKB for most participants was only taken once, and therefore can be prone to errors that a median of multiple measurements might buffer against. Both of the above factors would influence the estimation of the effect of rare genetic variants on IOP. Second, since a glaucoma diagnosis can often be made well after the onset of disease, we can expect that a certain percentage of controls have undiagnosed glaucoma, which may affect the effect size estimate. Third, the *ANGPTL7* gene in humans lies within intron 28 of *MTOR*³⁹, therefore variants in *ANGPTL7* could also affect *MTOR* function. While a possibility, it is unlikely that the effect on IOP and glaucoma is due to *MTOR*, as: (i) the variants are predicted to be protein-altering in *ANGPTL7* whereas there is no obvious predicted functional effect on *MTOR*; (ii) we show data suggesting that the variants have a functional impact on *ANGPTL7*; and (iii) we show mouse data that establish a role for *ANGPTL7* in IOP regulation.

In summary, our genetic and pharmacological results indicate that *ANGPTL7* participates in the normal physiological regulation of IOP in humans and mice. Since excessive amounts of mAngptl7 protein in the eyes of experimental animals cause IOP to elevate to pathological levels, upregulation of *ANGPTL7* in humans may be responsible for the elevated IOP that leads to POAG. Therefore, we propose *ANGPTL7* as an excellent candidate to explore as a therapeutic target for POAG.

Methods

Ethics approval and informed consent. All participants provided informed consent, and studies were approved by the individual IRBs at the respective institutions. UK Biobank has approval from the North West Multi-center Research Ethics Committee (MREC), which covers the UK. It also sought the approval in England and Wales from the Patient Information Advisory Group (PIAG) for gaining access to information that would allow it to invite people to participate. The DiscovEHR study was approved by the Institutional Review Board (IRB) at Geisinger. The BioMe Biobank is an ongoing research biorepository approved by the Icahn School of Medicine at Mount Sinai's IRB. The

Ethical Committee at Lund University approved the Malmo Diet and Cancer Study (LU 51–90) and all the participants provided a written informed consent. The CGPS study (H-KF-01-144/01) was approved by the Ethics Committee of the Capital Region and from the Danish Data Protection Agency. Research at Estonian Biobank is regulated by Human Gene Research Act and all participants have signed a broad informed consent. IRB approval for current study was granted by Research Ethics Committee of University of Tartu, approval nr 236/T-23. For the POAAGG study, approval to enroll and to recontact subjects was obtained from the University of Pennsylvania IRB. The FinnGen Biobank was evaluated and approved by the Coordinating Ethics Committee of the Helsinki and Uusimaa Hospital District.

Study design. Association with IOP was tested on a total of 101,678 individuals and 27,529 individuals of European ancestry from the United Kingdom Biobank (UKB) and the MyCode Community Health Initiative cohort from Geisinger Health System (GHS), respectively. The UKB is a population-based cohort study of people aged between 40 and 69 years recruited through 22 testing centers in the UK between 2006 and 2010⁴⁰. The GHS MyCode study is a health system-based cohort of patients from Central and Eastern Pennsylvania (USA) recruited in 2007–2019⁴¹. For IOP association tests in African ancestry individuals, we included 4114 individuals from UKB and 3167 individuals from the Primary Open Angle African-American Glaucoma Genetics (POAAGG) study conducted at the University of Pennsylvania Perelman School of Medicine⁴². We excluded all participants with a glaucoma diagnosis code (ICD-10 H40) or self-reported glaucoma (UKB field IDs: 6148 and 20002) from IOP analyses.

Association of *ANGPTL7* variants with glaucoma was tested in 8 studies: UKB, GHS, Mt. Sinai BioMe cohort (SINAI), the Malmö Diet and Cancer study (MALMO)⁴³, the Estonia Biobank (EstBB)⁴⁴, The Trøndelag Health Study (HUNT)⁴⁵, FinnGen, a study from Finland, and the Copenhagen General Population Study and the Copenhagen City Heart Study (CGPS-CCHS)⁴⁶. We had, in total, up to 40,042 cases (UKB: 12,377; GHS: 8032; SINAI: 409; MALMO: 2395; EstBB: 7629; HUNT: 3874; CPGS-CCHS: 1863; FinnGen: 3463) and 947,782 controls of European ancestry, and 5153 cases (UKB: 448, POAAGG: 3444, SINAI: 1261) and 21,650 controls of African ancestry in glaucoma analyses.

Phenotype definition. IOP in UKB was measured in each eye using the Ocular Response Analyzer (Reichert Corp., Buffalo, New York). Participants were excluded from this test if they reported having eye surgery in the preceding 4 weeks or having an eye infection. The Ocular Response Analyzer calculates two forms of IOP, a Goldmann-correlated IOP (IOPg) and a corneal-compensated IOP (IOPcc). IOPg most closely approximates the IOP measured by the Goldmann Applanation Tonometer (GAT), which has been the gold standard for measuring IOP, while IOPcc provides a measure of IOP that is adjusted to remove the influence of corneal biomechanics⁴⁷. For this study, we focused on IOPg as this measurement is the most comparable to IOP measurements in other cohorts, and herein IOPg will be referred to as IOP. IOP in POAAGG was measured using a GAT. In GHS, IOP measurements were obtained from several instruments including GAT, Tono-pen and I-Care, which are correlated with IOPg readings from the Ocular Response Analyzer⁴⁸. For GHS individuals who were not prescribed any IOP medications, we used the median of all IOP measurements available. For individuals who had an IOP medication prescribed, we used the median of IOP measurements available preceding the start date for IOP medications (if available). Individuals for whom we did not have non-medicated IOP values were excluded from the IOP genetic analyses. For association analyses of IOP, we excluded individuals with: (1) a glaucoma diagnosis; (2) IOP measures that were more than 5 standard deviations away from the mean; (3) more than a 10-mmHg difference between both eyes. We derived a mean IOP measure between both eyes for each individual. IOP of only one eye was used in instances where IOP measures for both eyes were not available.

Details on glaucoma definition in each cohort are given in the Supplementary Methods. In brief, glaucoma cases in GHS, SINAI, MALMO, HUNT, EstBB, FinnGen (v.R3) and CGPS-CCHS were defined by the presence of an ICD-10 H40 diagnosis code in either outpatient or inpatient electronic health records. In UKB, glaucoma cases were defined as individuals with either an ICD-10 H40 diagnosis or self-reported glaucoma (UKB field ID: 6148 or 20002). In the POAAGG cohort, glaucoma cases and controls were classified based on an ophthalmic examination by glaucoma specialists, and glaucoma suspects were also included in the cases⁴².

Statistics and reproducibility. High coverage whole exome sequencing and genotyping was performed at the Regeneron Genetics Center^{49,50} as described in Supplementary Methods. We estimated the association with IOP and glaucoma of genetic variants or their gene burden using REGENIE v1.0.43⁵¹ (UKB, GHS, MALMO, SINAI), SAIGE⁵² (HUNT, EstBB, FinnGen) or logistic regression (CGPS-CCHS). Analyses were adjusted for age, age², sex, an age-by-sex interaction term, experimental batch-related covariates, and genetic principal components, where appropriate. Cohort-specific statistical analysis details are provided in Supplementary Methods. Results across cohorts were pooled using inverse-variance weighted meta-analysis. Details on the PheWAS analysis conducted in UKB and GHS are provided in Supplementary Methods. Western blotting and ELISA analyses were repeated on three independent biological replicates and data are presented as mean ± SEM. Technical replicates ($n = 3$) were run for the ELISA analysis. P values were calculated by one-way ANOVA with Tukey's multiple comparison test for multiple groups analysis (Supplementary Data 1). A total of 12 eyes were used to test the effect of increasing mAngptl7 levels in mouse eyes and Student's t test was used to calculate the significance of the resulting change in IOP. The IOP was measured on 33 WT, 41 *Angptl7* KO and 15 *Angptl7* Het mice and conventional outflow facility was measured on 4 WT and 7 *Angptl7* KO mice. Unpaired Student's t -test was used to calculate the statistical significance of the results between the different genotypes. For in vivo siRNA knockdown of mAngptl7, we used 8, 6, 6 and 5 mouse eyes for siRNA#3, siRNA#5, PBS-treated and Naïve controls, respectively. Statistical significance was calculated using one-way ANOVA with Dunnett's post hoc analysis (Supplementary Data 1).

In vitro characterization. HEK293 cells, derived within Regeneron, were cultured in DMEM media 4.5 g/L D-Glucose, (+) L-Glutamine, (-) Sodium Phosphate, (-) Sodium Pyruvate supplemented with 10% FBS and 1% Penicillin-Streptomycin-Glutamine (Invitrogen), at 37 °C in a humidified atmosphere under 5% CO₂. The day before transfection, HEK293 cells were seeded in OptiMEM supplemented with 10% FBS. After 24 h, the cells were transfected with FuGENE 6, and 10 µg of pcDNA 3.1(+) encoding the following proteins: ANGPTL7 WT, Gln175His, Arg177* and Trp188*. After 24 h, the media was changed with 2% FBS OptiMEM. The following day, the cells were collected in RIPA buffer, supplemented with protease and phosphatase inhibitors (BRAND) or TRIZOL reagent (Invitrogen) for protein and RNA analysis, respectively. The supernatants were transferred to an Eppendorf tube and immediately flash frozen for downstream protein analysis. Western blot analysis was performed using a rabbit polyclonal antibody against ANGPTL7 at 1:1000 dilution (10396-1-AP ProteinTech), using standard procedures. ANGPTL7 was quantified by ELISA according to manufacturer's instructions (LS-F50425 Life Sciences). The cell lysates were diluted 1:1000. The supernatants were diluted 1:10,000. The ELISA plate was read at 450 nm via SpectraMax M4 plate reader (Molecular Devices).

Total RNA was extracted using TRIzol reagent (Invitrogen) and RNeasy kit (Qiagen) according to manufacturer's instructions and treated with RNase-free DNase I (Promega). cDNA was synthesized using Superscript VILO cDNA synthesis kit (Invitrogen). Taqman analysis was performed using TaqMan Fast Advanced Master Mix (Applied Biosystems) in a QuantStudio 6 Flex (Applied Biosystems) and commercially available primers and probes for ANGPTL7 (Hs00221727—Applied Biosystems) and GAPDH (Hs02786624_g1—Applied Biosystems).

In vivo characterization. All animal protocols were approved by the Institutional Animal Care and Use Committee in accordance with the Regeneron's Institutional Animal Care and Use Committee (IACUC) and the Association for Research in Vision and Ophthalmology (ARVO) Statement for the Use of Animals in Ophthalmic and Vision Research. *Angptl7*^{-/-} mice, on 63% C57BL/6NTac and 37% 129SvEvTac background, were generated by Regeneron Pharmaceuticals using the VelociMouse® technology⁵³. Heterozygous mice (*Angptl7*^{+/-}) were bred to generate age-matched wild-type, het and KO littermates that were used for experimentation at 3–4 months of age (mixed gender). Ocular anatomy in these mice was characterized using optical coherence tomography. Detailed methods on generation and characterization of KO mice are provided in Supplementary Methods. For in vivo siRNA experiments, we used C57BL/6J male mice, 3–4 months old, from Jackson Labs.

IOP measurements. Mice were anesthetized and IOP was measured in both eyes using a TonoLab rebound tonometer (Colonial Medical Supply, Franconia, NH) before the start of *Angptl7* injection and every day afterwards for six days^{54–56}. When testing *Angptl7* siRNAs, IOPs were measured in each eye before then start of experiment and then every week until end of study. IOP measurements for both eyes were completed within 3–5 min. Six correct single measurements were done on each eye to generate one IOP reading. We took five IOP readings for each eye and used the average of those readings at each time-point.

Aqueous humor outflow facility measurements. Aqueous humor outflow facility (C) was measured by using our constant flow infusion technique in live mice^{55–58}. Mice were anesthetized by using a 100/10 mg/kg ketamine/xylazine cocktail. A

quarter to half of this dose was administered for maintenance of anesthesia as necessary. One to two drops of proparacaine HCl (0.5%) (Bausch + Lomb) were applied topically to both eyes for corneal anesthesia. The anterior chambers of both eyes were cannulated by using a 30-gauge needle inserted through the cornea 1–2 mm anteriorly to the limbus and pushed across the anterior chamber to a point in the chamber angle opposite to the point of cannulation, taking care not to touch the iris, anterior lens capsule epithelium, or corneal endothelium. Each cannulating needle was connected to a previously calibrated (sphygmomanometer, Diagnostix 700; American Diagnostic Corporation, Hauppauge, NY, USA) flow-through BLPR-2 pressure transducer (World Precision Instruments [WPI], Sarasota, FL, USA) for continuous determination of pressure within the perfusion system. A drop of gentalin (Alcon) was also administered to each eye to prevent corneal drying. The opposing ends of the pressure transducer were connected via further tubing to a 1 ml syringe loaded into a microdialysis infusion pump (SP2001 Syringe Pump; WPI). The tubing, transducer, and syringe were all filled with sterile DPBS (Gibco). Signals from each pressure transducer were passed via a TBM4M Bridge Amplifier (WPI) and a Lab-Trax Analog-to-Digital Converter (WPI) to a computer for display on a virtual chart recorder (LabScribe2 software; WPI). Eyes were initially infused at a flow rate of 0.1 µl/min. When pressures stabilized within 10–30 min, pressure measurements were recorded over a 5-min period, and then flow rates were increased sequentially to 0.2, 0.3, 0.4, and 0.5 µl/min. Three stabilized pressures at 3-minute intervals at each flow rate were recorded. C in each eye of each animal was calculated as the reciprocal of the slope of a plot of mean stabilized pressure as ordinate against flow rate as abscissa.

Injection of *Angptl7* protein and siRNA into mouse eyes. A 33-gauge needle with a glass microsyringe (5-µl volume; Hamilton Company) was used for injections of *Angptl7* protein/siRNA into mice eyes. For intravitreal injections, the eye was proptosed, and the needle was inserted through the equatorial sclera and into the vitreous chamber at an angle of approximately 45 degrees, taking care to avoid touching the posterior part of the lens or the retina. *Angptl7* protein (catalog# 4960-AN-025; R&D Systems, Minneapolis, MN) or siRNA (from Alnylam Pharmaceuticals, Supplementary Methods) or PBS (1 µL) was injected into the vitreous over the course of 1 minute. The needle was then left in place for a further 45 s (to facilitate mixing), before being rapidly withdrawn. siRNA sequences for all six probes tested are provided in Table 2. Before and during intracameral injections of *Angptl7* protein, mice were anesthetized with isoflurane (2.5%) containing oxygen (0.8 L/min). For topical anesthesia, both eyes received one to two drops of 0.5% proparacaine HCl (Akorn Inc.). Each eye was proptosed and the needle was inserted through the cornea just above the limbal region and into the anterior chamber at an angle parallel to the cornea, taking care to avoid touching the iris, anterior lens capsule epithelium, or corneal endothelium. Up to 1 µL of *Angptl7* protein or PBS was injected into each eye over a 30-s period before the needle was withdrawn. Only one injection was administered at day 0.

Reporting summary. Further information on research design is available in the Nature Research Reporting Summary linked to this article.

Data availability

Source data underlying main figures are provided in Supplementary Data 1. Uncropped and unedited images of the blots that appear in the main article are provided in Supplementary Data 2. All whole exome sequencing, genotyping chip, and imputed sequence described in this report are publicly available to registered researchers via the UK Biobank data access protocol. Additional information about registration for access to the data is available at <http://www.ukbiobank.ac.uk/register-apply/>. Further information about the whole exome sequence is available at https://www.ukbiobank.ac.uk/media/kjmdwfg/access_064-uk-biobank-exome-release-faq_v10.pdf. Detailed information about the chip and imputed sequence is available at: <https://www.ukbiobank.ac.uk/media/cffi4mx5/ukb-genotyping-and-imputation-data-release-faq-v3-2-1.pdf>. DiscovEHR and the University of Pennsylvania exome sequencing and genotyping data can be made available to qualified, academic, non-commercial researchers upon request via a Data Transfer Agreement with Geisinger Health System and University of Pennsylvania, respectively. Genetic data for the HUNT, CGPS-CCHS and Estonia cohorts may be made available by contacting the respective institutions. FinnGen R3 data can be accessed at: <https://www.finnngen.fi/>. Regeneron materials described in this manuscript may be available to qualified academic researchers upon request through our portal (https://regeneron.envisionpharma.com/vt_regeneron/). In certain circumstances in which we are unable to provide a particular proprietary reagent, an alternative molecule may be provided that behaves in a similar manner. Additional information about how we share our materials can be obtained by contacting Regeneron's preclinical collaborations email address (preclinical.collaborations@regeneron.com).

Received: 3 September 2021; Accepted: 1 September 2022;
Published online: 03 October 2022

References

1. Tham, Y.-C. et al. Global prevalence of glaucoma and projections of glaucoma burden through 2040: a systematic review and meta-analysis. *Ophthalmology* **121**, 2081–2090 (2014).
2. Weinreb, R. N., Aung, T. & Medeiros, F. A. The pathophysiology and treatment of glaucoma: a review. *JAMA* **311**, 1901–1911 (2014).
3. Wolfs, R. C. et al. Genetic risk of primary open-angle glaucoma. Population-based familial aggregation study. *Arch. Ophthalmol.* **116**, 1640–1645 (1998).
4. Toh, T. et al. Central corneal thickness is highly heritable: the twin eye studies. *Invest. Ophthalmol. Vis. Sci.* **46**, 3718–3722 (2005).
5. Green, C. M. et al. How significant is a family history of glaucoma? Experience from the Glaucoma Inheritance Study in Tasmania. *Clin. Exp. Ophthalmol.* **35**, 793–799 (2007).
6. Marcus, M. W., de Vries, M. M., Junoy Montolio, F. G. & Jansonius, N. M. Myopia as a risk factor for open-angle glaucoma: a systematic review and meta-analysis. *Ophthalmology* **118**, 1989–1994.e2 (2011).
7. Hollands, H. et al. Do findings on routine examination identify patients at risk for primary open-angle glaucoma? The rational clinical examination systematic review. *JAMA* **309**, 2035–2042 (2013).
8. Asefa, N. G., Neustaeter, A., Jansonius, N. M. & Snieder, H. Heritability of glaucoma and glaucoma-related endophenotypes: Systematic review and meta-analysis. *Surv. Ophthalmol.* **64**, 835–851 (2019).
9. Landers, J. A. et al. Craig, Heritability of central corneal thickness in nuclear families. *Invest. Ophthalmol. Vis. Sci.* **50**, 4087–4090 (2009).
10. Carbonaro, F., Andrew, T., Mackey, D. A., Spector, T. D. & Hammond, C. J. Heritability of intraocular pressure: a classical twin study. *Br. J. Ophthalmol.* **92**, 1125–1128 (2008).
11. van Koolwijk, L. M. E. et al. Genetic contributions to glaucoma: heritability of intraocular pressure, retinal nerve fiber layer thickness, and optic disc morphology. *Invest. Ophthalmol. Vis. Sci.* **48**, 3669–3676 (2007).
12. Pärssinen, O. et al. Heritability of intraocular pressure in older female twins. *Ophthalmology* **114**, 2227–2231 (2007).
13. Healey, P. et al. The heritability of optic disc parameters: a classic twin study. *Invest. Ophthalmol. Vis. Sci.* **49**, 77–80 (2008).
14. Khawaja, A. P. et al. UK Biobank Eye and Vision Consortium, NEIGHBORHOOD Consortium, Genome-wide analyses identify 68 new loci associated with intraocular pressure and improve risk prediction for primary open-angle glaucoma. *Nat. Genet.* **50**, 778–782 (2018).
15. Gao, X. R., Huang, H., Nannini, D. R., Fan, F. & Kim, H. Genome-wide association analyses identify new loci influencing intraocular pressure. *Hum. Mol. Genet.* **27**, 2205–2213 (2018).
16. Choquet, H. et al. A large multi-ethnic genome-wide association study identifies novel genetic loci for intraocular pressure. *Nat. Commun.* **8**, 2108 (2017).
17. Garg, A. & Gazzard, G. Treatment choices for newly diagnosed primary open angle and ocular hypertension patients. *Eye* **34**, 60–71 (2020).
18. Patel, A. R. et al. Economic and Clinical Burden Associated With Intensification of Glaucoma Topical Therapy: A US Claims-based Analysis. *J. Glaucoma* **30**, 242–250 (2021).
19. Tanigawa, Y. et al. Rare protein-altering variants in ANGPTL7 lower intraocular pressure and protect against glaucoma. *PLoS Genet* **16**, e1008682 (2020).
20. Luce, D. A. Determining in vivo biomechanical properties of the cornea with an ocular response analyzer. *J. Cataract Refract. Surg.* **31**, 156–162 (2005).
21. Comes, N., Buie, L. K. & Borrás, T. Evidence for a role of angiopoietin-like 7 (ANGPTL7) in extracellular matrix formation of the human trabecular meshwork: implications for glaucoma. *Genes Cells* **16**, 243–259 (2011).
22. Kuchtey, J. et al. Angiopoietin-like 7 secretion is induced by glaucoma stimuli and its concentration is elevated in glaucomatous aqueous humor. *Invest. Ophthalmol. Vis. Sci.* **49**, 3438–3448 (2008).
23. Peek, R., Kammerer, R. A., Frank, S., Otte-Höller, I. & Westphal, J. R. The angiopoietin-like factor cornea-derived transcript 6 is a putative morphogen for human cornea. *J. Biol. Chem.* **277**, 686–693 (2002).
24. C. Carbone, et al, Angiopoietin-like proteins in angiogenesis, inflammation and cancer. *Int. J. Mol. Sci.* **19** (2018), <https://doi.org/10.3390/ijms19020431>.
25. Patel, G. et al. Molecular taxonomy of human ocular outflow tissues defined by single-cell transcriptomics. *Proc. Natl Acad. Sci. USA* **117**, 12856–12867 (2020).
26. van Zyl, T. et al. Cell atlas of aqueous humor outflow pathways in eyes of humans and four model species provides insight into glaucoma pathogenesis. *Proc. Natl Acad. Sci. USA* **117**, 10339–10349 (2020).
27. Bhattacharya, S. K. et al. Proteomics reveal Cochlin deposits associated with glaucomatous trabecular meshwork. *J. Biol. Chem.* **280**, 6080–6084 (2005).
28. Comes, N. & Borrás, T. Individual molecular response to elevated intraocular pressure in perfused postmortem human eyes. *Physiol. Genomics* **38**, 205–225 (2009).
29. Lo, W. R. et al. Tissue differential microarray analysis of dexamethasone induction reveals potential mechanisms of steroid glaucoma. *Invest. Ophthalmol. Vis. Sci.* **44**, 473–485 (2003).
30. Rozsa, F. W. et al. Gene expression profile of human trabecular meshwork cells in response to long-term dexamethasone exposure. *Mol. Vis.* **12**, 125–141 (2006).
31. Clark, A. F. Basic sciences in clinical glaucoma: steroids, ocular hypertension, and glaucoma. *J. Glaucoma* **4**, 354–369 (1995).
32. Phulke, S., Kaushik, S., Kaur, S. & Pandav, S. S. Steroid-induced glaucoma: an avoidable irreversible blindness. *J. Curr. Glaucoma Pr.* **11**, 67–72 (2017).
33. Wang, J. et al. Targeting transforming growth factor- β signaling in primary open-angle glaucoma. *J. Glaucoma* **26**, 390–395 (2017).
34. Garcia-Porta, N. et al. Corneal biomechanical properties in different ocular conditions and new measurement techniques. *ISRN Ophthalmol.* **2014**, 724546 (2014).
35. Gordon, R. A. & Donzis, P. B. Refractive development of the human eye. *Arch. Ophthalmol.* **103**, 785–789 (1985).
36. Fan, Q. et al. Genome-wide association meta-analysis of corneal curvature identifies novel loci and shared genetic influences across axial length and refractive error. *Commun. Biol.* **3**, 133 (2020).
37. Choquet, H. et al. A multiethnic genome-wide analysis of 44,039 individuals identifies 41 new loci associated with central corneal thickness. *Commun. Biol.* **3**, 301 (2019).
38. Stein, J. D., Khawaja, A. P. & Weizer, J. S. Glaucoma in adults-screening, diagnosis, and management: a review. *JAMA* **325**, 164–174 (2021).
39. Katoh, Y. & Katoh, M. Comparative integromics on angiotensin family members. *Int. J. Mol. Med.* **17**, 1145–1149 (2006).
40. Sudlow, C. et al. UK biobank: an open access resource for identifying the causes of a wide range of complex diseases of middle and old age. *PLoS Med.* **12**, e1001779 (2015).
41. Carey, D. J. et al. The Geisinger MyCode community health initiative: an electronic health record-linked biobank for precision medicine research. *Genet. Med.* **18**, 906–913 (2016).
42. Charlson, E. S. et al. The primary open-angle African American glaucoma genetics study: baseline demographics. *Ophthalmology* **122**, 711–720 (2015).
43. Berglund, G., Elmstahl, S., Janzon, L. & Larsson, S. A. Design and feasibility *J. Internal Med.* **233**, 45–51 (1993).
44. Leitsalu, L. et al. Cohort Profile: Estonian Biobank of the Estonian Genome Center, University of Tartu. *Int. J. Epidemiol.* **44**, 1137–1147 (2015).
45. Krokstad, S. et al. Cohort profile: The HUNT study, Norway. *Int. J. Epidemiol.* **42**, 968–977 (2013).
46. Aguib, Y. & Al Suwaidi, J. The Copenhagen city heart study (Østerbroudersøgelsen). *Glob. Cardiol. Sci. Pract.* **2015**, 33 (2015).
47. Luce, D. Methodology for cornea compensated IOP and corneal resistance factor for the reichert ocular response analyzer. *Invest. Ophthalmol. Vis. Sci.* **47**, 2266–2266 (2006).
48. Eriksson, E., Davidsson, L. & Brautaset, R. A comparative study of the tonometers: Goldmann applanation, Perkins, Tono-Pen XL and Reichert 7CR. *Int. J. Ophthalmic Pract.* **2**, 246–251 (2011).
49. Dewey, F. E. et al. Distribution and clinical impact of functional variants in 50,726 whole-exome sequences from the DiscovEHR study. *Science* **354**, aaf6814 (2016).
50. Van Hout, C. V. et al. Exome sequencing and characterization of 49,960 individuals in the UK Biobank. *Nature* **586**, 749–756 (2020).
51. Mbatshou, J. et al. Computationally efficient whole-genome regression for quantitative and binary traits. *Nat. Genet.* <https://doi.org/10.1038/s41588-021-00870-7> (2021).
52. Zhou, W. et al. Efficiently controlling for case-control imbalance and sample relatedness in large-scale genetic association studies. *Nat. Genet.* **50**, 1335–1341 (2018).
53. DeChiara, T. M. et al. VelociMouse: fully ES cell-derived F0-generation mice obtained from the injection of ES cells into eight-cell-stage embryos. *Methods Mol. Biol.* **530**, 311–324 (2009).
54. Wang, W.-H., Millar, J. C., Pang, I.-H., Wax, M. B. & Clark, A. F. Noninvasive measurement of rodent intraocular pressure with a rebound tonometer. *Invest. Ophthalmol. Vis. Sci.* **46**, 4617–4621 (2005).
55. Patel, G. C., Millar, J. C. & Clark, A. F. Glucocorticoid receptor transactivation is required for glucocorticoid-induced ocular hypertension and glaucoma. *Invest. Ophthalmol. Vis. Sci.* **60**, 1967–1978 (2019).
56. Patel, G. C. et al. Dexamethasone-induced ocular hypertension in mice: Effects of myocilin and route of administration. *Am. J. Pathol.* **187**, 713–723 (2017).
57. Millar, J. C., Clark, A. F. & Pang, I.-H. Assessment of aqueous humor dynamics in the mouse by a novel method of constant-flow infusion. *Invest. Ophthalmol. Vis. Sci.* **52**, 685–694 (2011).
58. Patel, G. C., Liu, Y., Millar, J. C. & Clark, A. F. Glucocorticoid receptor GR β regulates glucocorticoid-induced ocular hypertension in mice. *Sci. Rep.* **8**, 862 (2018).

Acknowledgements

We would like to thank everyone who made this work possible. In particular: the UK Biobank team, their funders, the dedicated professionals from the member institutions who contributed to and supported this work, and most especially the UK Biobank participants, without whom this research would not be possible. The exome sequencing was funded by the UK Biobank Exome Sequencing Consortium (i.e., Bristol Myers Squibb, Regeneron, Biogen, Takeda, AbbVie, Alnylam, AstraZeneca and Pfizer). This research has been conducted using the UK Biobank Resource under application number 26041; EstBB, we thank all participants and staff of the Estonian biobank for their contribution to this research and the analytical work of EstBB was carried out in part in the High Performance Computing Center of the University of Tartu. L.M and K.K were supported by grants from the Estonian Research Council PRG184 and by the European Union through the European Regional Development Fund (Project No. 2014-2020.4.01.15-0012); We want to acknowledge the participants and investigators of the FinnGen study. We also thank the MyCode Community Health Initiative participants for taking part in the DiscovEHR collaboration. This research received funding from Regeneron Pharmaceuticals. JOB was supported by the National Eye Institute (#R01EY023557-01), Vision Research Core Grant (P30 EY001583), and NIH Grant (LM010098). Funds also come from the F.M. Kirby Foundation, Research to Prevent Blindness, The UPenn Hospital Board of Women Visitors, and The Paul and Evanina Bell Mackall Foundation Trust. The Ophthalmology Department at the Perelman School of Medicine and the VA Hospital in Philadelphia, Pennsylvania, also provided support. The funders had no role in study design, data collection and analysis, decision to publish, or preparation of the manuscript. The Trøndelag Health Study (The HUNT Study) is a collaboration between HUNT Research Center (Faculty of Medicine and Health Sciences, NTNU, Norwegian University of Science and Technology), Trøndelag County Council, Central Norway Regional Health Authority, and the Norwegian Institute of Public Health. The genotyping in HUNT was financed by the National Institutes of Health; University of Michigan; the Research Council of Norway; the Liaison Committee for Education, Research and Innovation in Central Norway; and the Joint Research Committee between St Olav's hospital and the Faculty of Medicine and Health Sciences, NTNU. S.S received funding from the Independent Research Fund, Denmark (Sapere Aude Research leader, grant number 9060-00012B). V.R.M.C received funding from R21EY028273-01A1 and the Lisa Dean Moseley Foundation Grant.

Author contributions

All authors contributed to critical review of the manuscript for important intellectual content, and final approval of submission of the manuscript for publication. Conceptualization: K.P., G.P., A.B., C.R., and G.C. Data curation: D.L., M.N.C. Genetic Analysis: K.P., L.G., M.A.F., A.H.A., S.A.D.G., A.L., T.M.T., C.S., D.S., K.K., B.B., S.S., E.S., E.J. Funding acquisition: G.D.Y., G.R.A., A.B., J.M.B., C.R., L.M., O.M., S.S., K.H. Mouse experiments: G.P., B.P. S.W., H.Y., W.F., S.Z., J.S.R., W.F. siRNA design and development: S.L., J.M., S.Waldron, S.H. In vitro experiments: G.D.G., T.P., L.M., M.D.S. Project administration: E.C., M.B.J. Datasets: J.M.B., V.R.M.C., H.V.G., R.S., B.B., K.H., B.O.A., C.W., K.K., L.M., S.S., A.S., A.T., O.M. Supervision: M.A.F., G.D.G., Y.H., K.H., L.M., K.K., A.E., J.W., A.B., C.R., G.C. Writing—original draft: K.P., G.P., G.D.G., T.V.Z., C.R., G.C. All authors contributed to securing funding, study design and oversight. All authors reviewed the final version of the manuscript (RGC Management and Leadership Team). C.B., C.F., A.L., and J.D.O. performed and are responsible for sample genotyping. C.B., C.F., E.D.F., M.L., M.S.P., L.W., S.E.W., A.L., and J.D.O. performed and are responsible for exome sequencing. T.D.S., Z.G., A.L., and J.D.O. conceived and are responsible for laboratory automation. M.S.P., K.M., R.U., and J.D.O. are responsible for

sample tracking and the library information management system. X.B., A.H., O.K., A.M., S.O., R.P., T.P., A.R., W.S. and J.G.R. performed and are responsible for the compute logistics, analysis and infrastructure needed to produce exome and genotype data. G.E., M.O., M.N. and J.G.R. provided compute infrastructure development and operational support. S.B., S.Ba, S.C., K.S., S.K., and J.G.R. provided variant and gene annotations and their functional interpretation of variants. E.M., R.L., B.B., A.B., L.H., J.G.R. conceived and are responsible for creating, developing, and deploying analysis platforms and computational methods for analyzing genomic data. All authors contributed to the clinical informatics of the project (Clinical Informatics). All authors contributed to the analytical analysis of the project (Translational and Analytical Genetics). All authors contributed to the management and coordination of all research activities, planning and execution. All authors contributed to the review process for the final version of the manuscript (Research Program Management).

Competing interests

The authors declare the following competing interests: Regeneron authors receive salary from and own options and/or stock of the company. C.W.'s spouse is an employee of the Regeneron Genetics Center. The remaining authors declare no competing interests.

Additional information

Supplementary information The online version contains supplementary material available at <https://doi.org/10.1038/s42003-022-03932-6>.

Correspondence and requests for materials should be addressed to Aris Baras, Carmelo Romano or Giovanni Coppola.

Peer review information *Communications Biology* thanks Saidas Nair, Lulin Huang and the other anonymous reviewer(s) for their contribution to the peer review of this work. Primary Handling Editors: Eve Rogers. Peer reviewer reports are available.

Reprints and permission information is available at <http://www.nature.com/reprints>

Publisher's note Springer Nature remains neutral with regard to jurisdictional claims in published maps and institutional affiliations.





Open Access This article is licensed under a Creative Commons Attribution 4.0 International License, which permits use, sharing, adaptation, distribution and reproduction in any medium or format, as long as you give appropriate credit to the original author(s) and the source, provide a link to the Creative Commons license, and indicate if changes were made. The images or other third party material in this article are included in the article's Creative Commons license, unless indicated otherwise in a credit line to the material. If material is not included in the article's Creative Commons license and your intended use is not permitted by statutory regulation or exceeds the permitted use, you will need to obtain permission directly from the copyright holder. To view a copy of this license, visit <http://creativecommons.org/licenses/by/4.0/>.

© The Author(s) 2022


¹Regeneron Genetics Center, Tarrytown, NY 10591, USA. ²Regeneron Pharmaceuticals, Inc., Tarrytown, NY 10591, USA. ³K.G. Jebsen Center for Genetic Epidemiology, Department of Public Health and Nursing, NTNU, Norwegian University of Science and Technology, 7030 Trondheim, Norway. ⁴HUNT Research Center, Department of Public Health and Nursing, NTNU, Norwegian University of Science and Technology, 7600 Levanger, Norway. ⁵Clinic of Medicine, St. Olavs Hospital Trondheim University Hospital, 7030 Trondheim, Norway. ⁶Estonian Genome Centre, Institute of Genomics, University of Tartu, Tartu, Estonia. ⁷Department of Endocrinology, Clinic of Medicine, St. Olavs Hospital, Trondheim University Hospital, 7030 Trondheim, Norway. ⁸Department of Ophthalmology, Pearlman School of Medicine, University of Pennsylvania, Philadelphia, PA, USA. ⁹Alnylam Pharmaceuticals, Inc, Cambridge, MA 02142, USA. ¹⁰Bayer AG, Pharmaceuticals, Research and Development, 13342 Berlin, Germany. ¹¹Department of Clinical Biochemistry, Rigshospitalet, Copenhagen University Hospital, Copenhagen, Denmark. ¹²Division of Cardiovascular Medicine, Department of Internal Medicine, University of Michigan, Ann Arbor, MI, USA. ¹³Department of Computational Medicine and Bioinformatics, University of Michigan, Ann Arbor, MI, USA. ¹⁴Department of Human Genetics, University of Michigan, Ann Arbor, MI, USA. ¹⁵Lund University, Department of Clinical Sciences Malmö, Malmö, Sweden. ¹⁶Skåne University Hospital, Department of Emergency and Internal Medicine, Malmö, Sweden. *Lists of authors and their affiliations appear at the end of the paper. ✉email: aris.baras@regeneron.com; carl.romano@regeneron.com; giovanni.coppola@regeneron.com



Regeneron Genetics Center

RGC Management and Leadership Team Goncalo R. Abecasis¹, Aris Baras¹ [✉], Michael Cantor¹, Giovanni Coppola¹ [✉], Andrew Deubler¹, Aris Economides¹, Luca A. Lotta¹, John D. Overton¹, Jeffrey G. Reid¹, Alan Shuldiner¹, Katia Karalis¹ & Katherine Siminovitch¹

Sequencing and Lab Operations Christina Beechert¹, Caitlin Forsythe¹, Erin D. Fuller¹, Zhenhua Gu¹, Michael Lattari¹, Alexander Lopez¹, John D. Overton¹, Thomas D. Schleicher¹, Maria Sotiropoulos Padilla¹, Louis Widom¹, Sarah E. Wolf¹, Manasi Pradhan¹, Kia Manoochehri¹ & Ricardo H. Ulloa¹

Genome Informatics Xiaodong Bai¹, Suganthi Balasubramanian¹, Suying Bao¹, Boris Boutkov¹, Siying Chen¹, Gisu Eom¹, Lukas Habegger¹, Alicia Hawes¹, Shareef Khalid¹, Olga Krasheninina¹, Rouel Lanche¹, Adam J. Mansfield¹, Evan K. Maxwell¹, Mona Nafde¹, Sean O’Keeffe¹, Max Orelus¹, Razvan Panea¹, Tommy Polanco¹, Ayesha Rasool¹, Jeffrey G. Reid¹, William Salerno¹ & Kathie Sun¹

Clinical Informatics Amelia Averitt¹, Nilanjana Banerjee¹, Michael Cantor¹, Dadong Li¹ [✉], Sameer Malhotra¹, Deepika Sharma¹, Jeffery C. Staples¹ & Ashish Yadav¹

Translational and Analytical Genetics Goncalo R. Abecasis¹, Joshua Backman¹, Amy Damask¹, Lee Dobbyn¹, Manuel Allen Revez Ferreira¹, Arkopravo Ghosh¹, Christopher Gillies¹, Lauren Gurski¹, Eric Jorgenson¹ [✉], Hyun Min Kang¹, Michael Kessler¹, Jack Kosmicki¹, Alexander Li¹, Nan Lin¹, Daren Liu¹, Adam Locke¹, Jonathan Marchini¹, Anthony Marcketta¹, Joelle Mbatchou¹, Arden Moscati¹, Charles Paulding¹, Carlo Sidore¹, Eli Stahl¹ [✉], Kyoko Watanabe¹, Bin Ye¹, Blair Zhang¹ & Andrey Ziyatdinov¹

Research Program Management Esteban Chen¹, Marcus B. Jones¹, Michelle G. LeBlanc¹, Jason Mighty¹, Lyndon J. Mitnau¹, Nirupama Nishtala¹ & Nadia Rana¹

GHS-RGC DiscovEHR Collaboration

Lance J. Adams¹⁷, Jackie Blank¹⁷, Dale Bodian¹⁷, Derek Boris¹⁷, Adam Buchanan¹⁷, David J. Carey¹⁷, Ryan D. Colonie¹⁷, F. Daniel Davis¹⁷, Dustin N. Hartzel¹⁷, Melissa Kelly¹⁷, H. Lester Kirchner¹⁷, Joseph B. Leader¹⁷, David H. Ledbetter¹⁷, J. Neil Manus¹⁷, Christa L. Martin¹⁷, Raghu P. Metpally¹⁷, Michelle Meyer¹⁷, Tooraj Mirshahi¹⁷, Matthew Oetjens¹⁷, Thomas Nate Person¹⁷, Christopher Still¹⁷, Natasha Strande¹⁷, Amy Sturm¹⁷, Jen Wagner¹⁷ & Marc Williams¹⁷

¹⁷Geisinger, Danville, PA 17821, USA.

Estonian Biobank Research Team

Andres Metspalu⁶, Mari Nelis⁶, Reedik Mägi⁶ & Tõnu Esko⁶